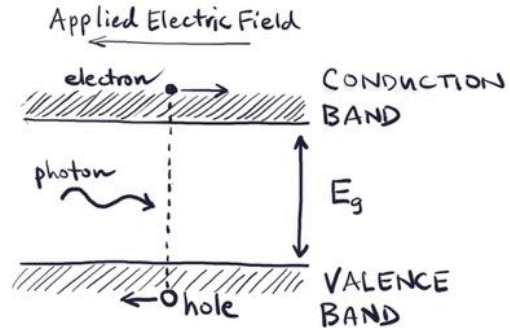


5. Detection of Infrared Radiation

5.1 Photoconductors

Most infrared detectors in use today are photoconductors or photodiodes using semiconductor materials. The semiconductor material produces free charge carriers when photons of sufficient energy hits the detector. The minimum energy to generate charges is determined by the band gap (E_g) of the semiconductor. This diagram illustrates the energy level diagram of a semiconductor. Photons with an energy greater than the band gap energy can move an electron into the conduction band.



The band gap energy is given in electron volts. Then the longest wavelength that can be detected is given by $\lambda_c = hc/E_g = 1.24 \mu\text{m} / E_g$, where λ_c is the cutoff wavelength and E_g is given in electron volts.

Notes:

Semiconductors are materials with electrical resistivities that are in between conductors and insulators.

Type	Resistivity, Ohm m	Resistance, Ohm (1mm length)
Conductor	10^{-8}	10^{-5}
Semiconductor	$10^{-2} - 10^2$	$10 - 10^4$
Insulator	10^8	10^{11}

At 0 K all of the electrons in the semiconductor are attached to the respective nuclei; thus there are no free electrons to contribute to current flow. Another way of expressing this is to say that all of the electrons are in the valence band and the conductivity is zero.

The distribution of electron energy is given by the Fermi-Dirac distribution.

McLean, I. (2008). *Electronic Imaging in Astronomy: Detectors and Instrumentation*, 2nd edition. New York, Springer.

Rieke, G. H. (2003). *Detection of Light: From the Ultraviolet to the Submillimeter*. Cambridge, Cambridge University Press.

Rieke, G. H. (2007). "Infrared Detector Arrays for Astronomy." *Annual Review of Astronomy and Astrophysics* **45**: 77-115.

For silicon, the band gap is 1.1 eV, so the longest wavelength that can be detected is 1.13 μm . The cut-off wavelength some important *intrinsic* photoconductors are shown here:

Material	Cutoff Wavelength (μm)
HgCdTe	0.8 to > 20
Si	1.1
Ge	1.6
InSb	5.5

Indium antimonide, with a 5.5 μm cutoff, and mercury cadmium telluride (HgCdTe) are often used in near-infrared astronomy. For HgCdTe, the band gap can be adjusted by varying the fraction x of the cadmium vs. mercury in the material ($\text{Hg}_{(1-x)}\text{Cd}_x\text{Te}$).

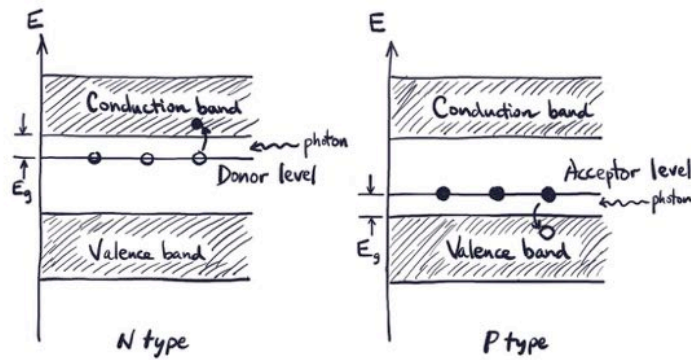
Since thermal excitation can also kick electrons into the conduction band (and create a dark current), the semiconductor material must be cooled to reduce this. A smaller band gap (longer cutoff wavelength) requires a colder temperature. The required cooling is approximated by $T_{\text{max}} = 200 \text{ K} / \lambda_c (\mu\text{m})$ (Rieke 2007). An InSb detector would require cooling to 36 K or less, for example.

Notes: The term *intrinsic* means the material is pure and the properties measured are intrinsic to the material. Table is from Bratt, P.R. 1977, in Semiconductors and Semimetals, vol. 12, ed. R.K. Willardson & A.C. Beer (New York: Academic), 39.

Reference: Rieke, G. H. (2007). "Infrared Detector Arrays for Astronomy." *Annual Review of Astronomy and Astrophysics* **45**: 77-115.

The number of electrons jumping into the conduction band proportional to $\exp(-E_g/2kT)$, where E_g is the energy gap and T is the temperature.

Smaller band gaps can be achieved by adding other elements into the semiconductor material. These added materials (dopants) can have one more or one less valence electron than silicon or germanium and are thus designated as p type or n type. The energy level diagram for the two types of materials is shown below. The donor and acceptor levels are close to the conduction and valence bands, and so less energy is required to excite an electron into the conduction band or a hole into the valence band. The photoconductor is designated as *extrinsic*, since its properties are determined by an added material.



Notes:

The different types of dopants used is shown here (Bratt 1977).

Material	Dopant	Type	Cutoff Wavelength (μm)
Si	Ga	p	17
Si	As	n	23
Si	B	p	28
Si	Sb	n	29
Ge	Be	p	52
Ge	Ga	p	115
Ge	Sb	n	129

Extrinsic photoconductors with dopants in both silicon and germanium have been successfully used at wavelengths as long as 200 μm in astronomy, notably on the *IRAS*, *ISO*, *Spitzer*, and *Herschel* missions.

Notes:

At 0 K all of the electrons are attached to the respective nuclei; thus there are no free electrons to contribute to current flow. Another way of expressing this is to say that all of the electrons are in the valence band and the conductivity is zero.

The distribution of electron energy is given by the Fermi-Dirac distribution:

$$P(E_n) = \frac{1}{\exp\left(\frac{E_n - E_F}{kT}\right) + 1}$$

where E_n is the energy of the thermally excited electron and E_F is the energy of the Fermi level. E_F is the energy level at which the probability of being occupied is 50%.

In order to keep the thermally excited electrons from entering the conduction band, we need to cool the detectors. Empirically the maximum temperature of the detector should be:

$$T_{max} = \frac{200 K}{\lambda_c(\mu m)}$$

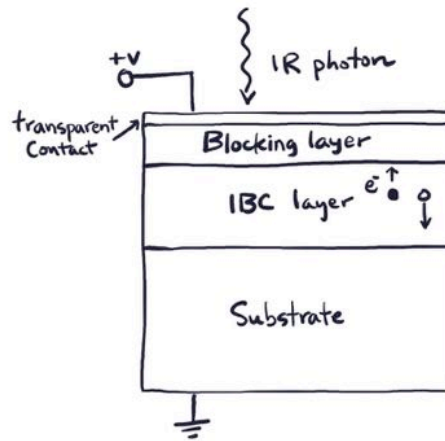
where λ_c is the long wavelength cutoff of the detector.

5-5

Notes:

From ~ 10 to $40 \mu\text{m}$, the impurity band conduction (IBC) detectors are the most sensitive. They are also known as the blocked impurity band (BIB) detector. These detectors have the advantage over extrinsic photoconductors by using a highly doped layer for greater quantum efficiency. The high dark current that normally would exist is blocked by a thin layer of intrinsic material at the contact. These detectors also have a longer cutoff wavelength than an extrinsic photoconductor of the same material.

Schematic of an IBC detector. The IBC layer is the layer where electrons are excited into the conduction band. The blocking layer of intrinsic material prevents the injection of holes from the transparent contact is prevented by the blocking layer. This allows very low dark current to be achieved.



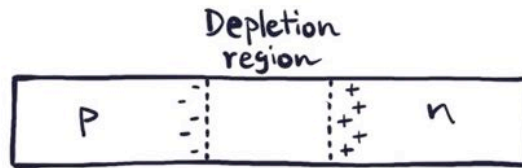
5-6

Notes:

References: Ives, D. et al. (2012). AQUARIUS, the next generation mid-IR detector for ground-based astronomy. *High Energy, Optical, and Infrared Detectors for Astronomy V*, SPIE, **8453**.
Bharat, R. (1994). "Impurity band conduction detectors for astronomy." *Experimental Astronomy* **3**: 219-225.

5.2 Photodiodes

While in principle it is possible to make sensitive infrared detectors using simple photoconductors, practical modern direct detectors use more complicated structures. For the intrinsic photoconductors, the detectors are almost always made as photodiodes, where n-doped material forms a junction with p-doped material. By forming a p-n junction, a charge-free region, the depletion region, is formed, and any photo-excited charge carriers formed in this region are swept to the contacts by the electric field in the region. This generates a current. The separation of charges across the depletion region creates a voltage of 0.6 V for silicon and 0.3 V for germanium.



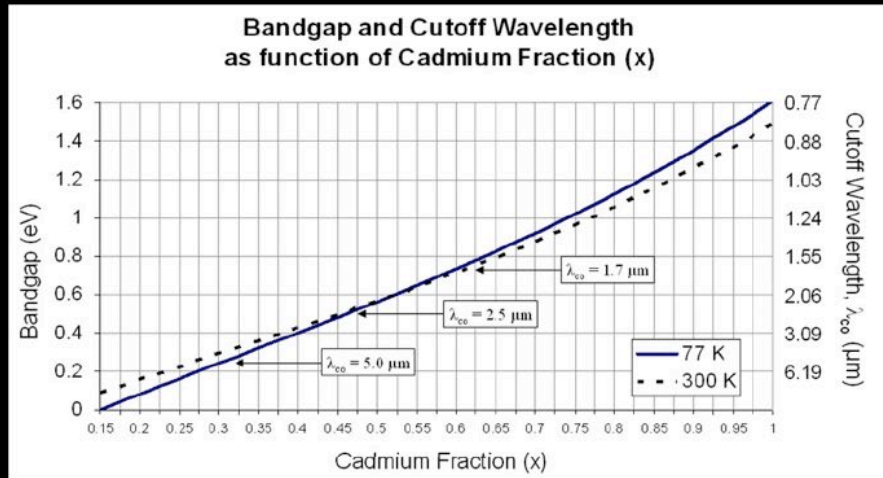
Photodiodes using InSb and HgCdTe are the most important intrinsic photodiodes in the near-infrared regime. High-performance photodiodes have been fabricated with HgCdTe for wavelengths as long as 10 μm .

Notes: See Rieke (2007) for description of the construction of a detector.

The photodiode is the basis for near-infrared detectors such as InSb and HgCdTe.

Tunable Wavelength: Valuable property of HgCdTe

$\text{Hg}_{1-x}\text{Cd}_x\text{Te}$ Modify ratio of Mercury and Cadmium to "tune" the bandgap energy



$$E_g = -0.302 + 1.93x - 0.81x^2 + 0.832x^3 + 5.35 \times 10^{-4} T(1 - 2x)$$

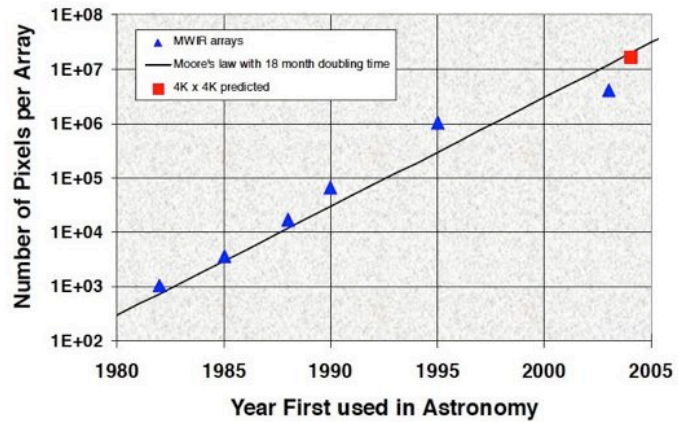
G. L. Hansen, J. L. Schmidt, T. N. Casselman, J. Appl. Phys. 53(10), 1982, p. 7099

Notes: Figure showing how the long wavelength cut off for HgCdTe can be modified by changing the cadmium fraction in the material.

5.3 Detector Arrays

There have been tremendous advances in the development of infrared arrays since 1980. This figure from Hoffman et al. (2004) shows the growth in the numbers of pixels per array in the near infrared. It shows a roughly 18 month doubling time.

The red square shows a 4Kx4K array, expected by 2005 but which was produced in 2008.



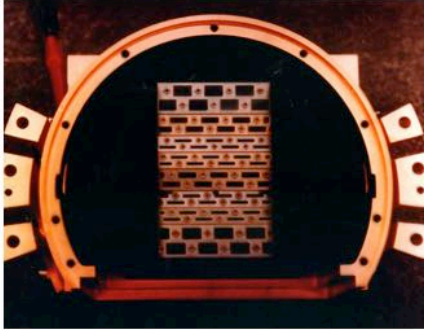
A. Tokunaga, Introduction to Infrared Astronomy, Univ. of Tokyo
Visiting Professor Lecture, Feb. 2018

5-9

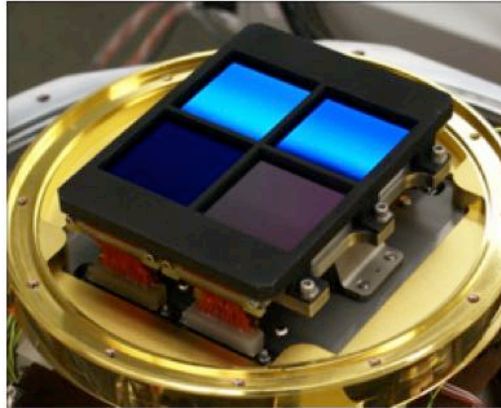
Notes: Although a 4Kx4K array was predicted to be achieved about 2004, such engineering-grade arrays were not achieved until 2012 and science-grade arrays about 2015 (D. Hall). This indicates that the practical limits of achieving ever larger arrays has been reached. The high cost of fabricating these arrays is also a factor and very few projects need or can afford larger infrared arrays.

Reference: Hoffman, A. W. et al. (2004). Megapixel detector arrays: visible to 28 μm . *Focal Plane Arrays for Space Telescopes*. SPIE, **5167**: 194-203.

A good illustration of the advances is to compare the *IRAS* focal plane array which had 62 detectors, with one of the focal plane arrays for the *JWST* NIRCam instrument, which has 16 million pixels. The entire NIRCam instrument alone has 40 million pixels.



IRAS focal plane with discrete detectors.



JWST NIRCam focal plan with four 1Kx1K HgCdTe detector arrays.

5-10

Notes:

The H2RG array.

The HAWAII 2RG array is used in instruments at many ground-based and space observatories. The acronym stands for “HgCdTe Astronomy Wide Area Infrared Imager” The “2” indicates this is a 2048^2 array. There are also 1024^2 and 4096^2 versions. The “R” indicates the array has reference pixels for removal of small electrical instabilities in the circuit such as a drift in voltage with time. The “G” stands for guide and it indicates that a small subarray of pixels can be read out for guiding.

The acronym HAWAII was chosen since the development of this line of detector arrays is led by a small group at the Institute for Astronomy and the Univ. of Hawaii. The principal investigator is Donald Hall (ref.).

What follows is a top-level description of this array and how it works. This will illustrate many of the technologies that are relevant to modern infrared arrays.

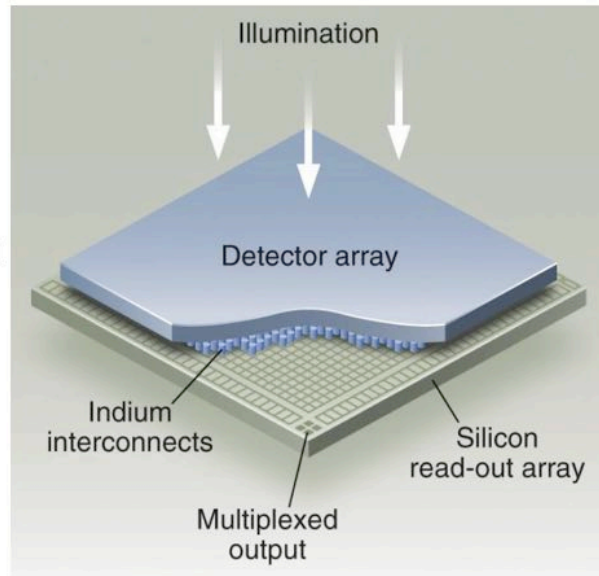
Notes:

Detailed discussion of H2RG arrays. Readout, noise, QE.

Nearly perfect detector.

Use in ground-based and space observatories.

This figure illustrates the principal architecture used on large-format detector arrays. Using integrated circuit technology, a readout circuit is fabricated out of silicon, one per detector element (pixel). There is also a multiplexing circuit to send the signals down a small number of output lines. The inputs to each amplifier are arranged in a grid on the top of the integrated circuit. The detector array is constructed out of the appropriate material for infrared absorption and carrier generation such as an array of photodiodes fabricated out of HgCdTe or an array of IBC detectors on a silicon substrate. The outputs of the detectors are connected to the readout circuit with indium bump bonds. These exactly matched microscopic indium bumps are deposited on both the detector array and the readout circuit. When the two sets of bumps are aligned and pressed together, a cold weld is formed in the indium and provides an electrical connection.



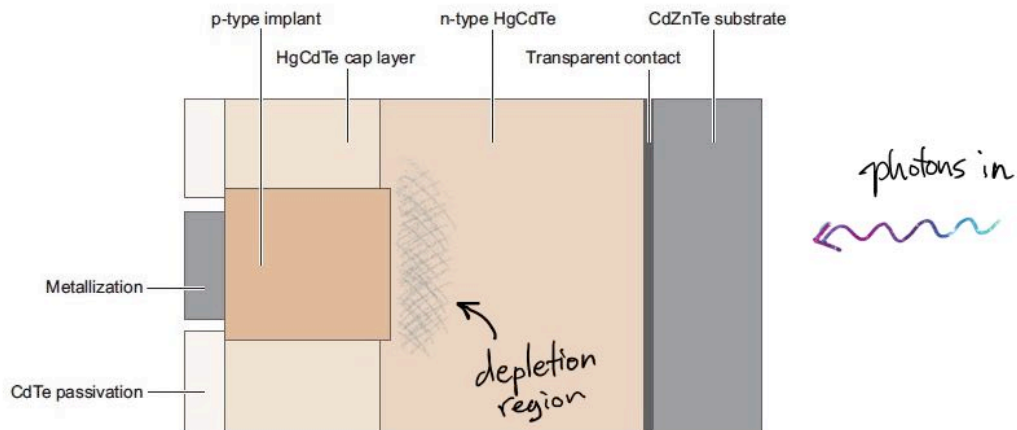
5-12

Notes: Figure from Beletic et al. (2008) illustrating the technique of bonding a detector array to a readout circuit. Unlike a CCD, each pixel is connected to an amplifier to detect and readout the charge. The reason for this approach is that the readout circuit is constructed out of silicon, while the detector material is made from InSb or HgCdTe. A CCD, on the other hand, can be constructed entirely out of silicon.

Indium is used for the electrical connection because it is a soft material and is electrically conducting at low temperatures.

Reference: Beletic, J. W. et al. (2008). Teledyne Imaging Sensors: infrared imaging technologies for astronomy and civil space. High Energy, Optical, and Infrared Detectors for Astronomy III., SPIE, **7021**, 70210H.

The detector array is composed of an array of photodiodes as shown in this figure (from Rieke 2007). In this example the photodiodes are made from p and n-type HgCdTe material. The metallic contact is used to create the electrical contact with the indium bump. Infrared photons pass through a CdZnTe substrate and a transparent contact to reach the depletion region where the photons are absorbed and charge carriers are generated.



5-13

Notes: This schematic diagram shows one pixel (one photodiode) of the array and gives you an idea of the complexity of the array construction. The pixel is connected electrically to the readout electronics by an indium bump that is pressed onto the metal contact shown on the left.

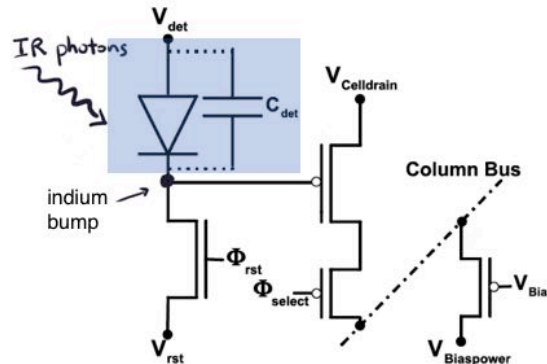
The active area is only about 10-15 micrometers thick. The substrate is thinned to maximize throughput.

Reference: Rieke, G. H. (2007). "Infrared Detector Arrays for Astronomy." *Annual Review of Astronomy and Astrophysics* 45: 77-115.

This schematic illustrates a simplified version of the readout electronics for one pixel (Rauscher 2015). The readout electronics for the entire detector array is known as the Readout Integrated Circuit (ROIC) and is *much* more complex than shown in this simplified diagram.

In order to determine the signal strength, a voltage is first applied across the inherent capacitance of the photodiode, C_{det} . The photodiode generates a current when illuminated and this discharges C_{det} . The change in voltage across C_{det} is a measure of the signal.

The voltage across C_{det} is measured with a MOSFET source follower amplifier (this amplifier converts a current into a voltage). The output voltage is read out along the column bus to which all the pixels in a column are attached to.



A. Tokunaga, Introduction to Infrared Astronomy, Univ. of Tokyo
Visiting Professor Lecture, Feb. 2018

5-14

Notes: Reference: Rauscher, B. J. (2015). "Teledyne H1RG, H2RG, and H4RG Noise Generator." Publications of the Astronomical Society of the Pacific **127**: 1144.

In this diagram the photodiode is shown using the standard symbol of a diode plus a "parasitic" capacitor inherent in any diode. The MOSFET (metal oxide semiconductor field effect transistors) in the circuit are used as switches and as a source follower amplifier. Φ_{rst} and Φ_{select} are switches to control the reset voltage applied to the detector and the selection of the detector for reading out.

The light blue square represents the photodiode. The location of the indium bump that establishes the electrical connection to the multiplexer is shown.

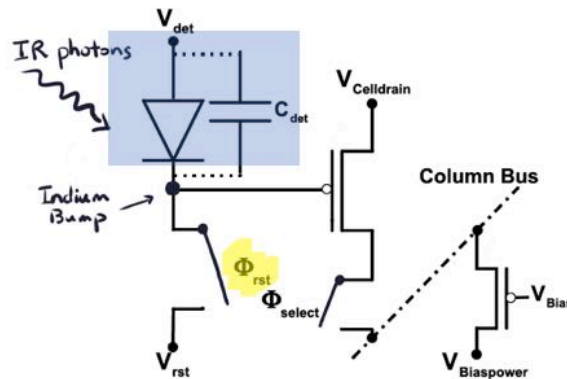
Since MOSFET transistors are used, the signal level can be measured non-destructively. This is a significant factor that allows for the reduction of noise.

Φ_{rst} and Φ_{select} are MOSFET switches.
This diagram shows this explicitly.

When Φ_{rst} is switched on and off, a voltage V_{det} is applied across the photodiode (assume V_{rst} is set to zero volts). This voltage remains across the photodiode since the circuit is open and it is the charge across C_{det} .

When the photodiode is illuminated by IR photons, a current is generated that discharges C_{det} . The change in voltage across C_{det} is a direct measure of the signal.

Note, however, that C_{det} varies with voltage across the photodiode junction, so it is not a constant. This leads to a non-linearity as it discharges to zero volts.

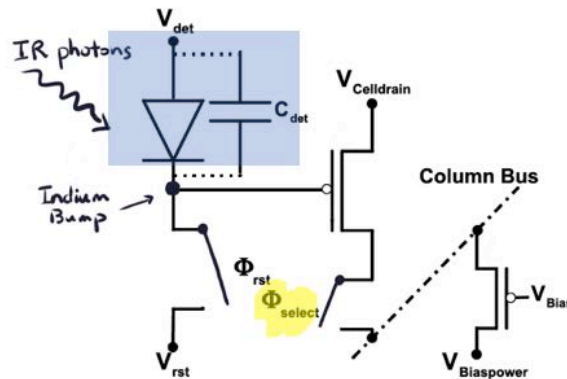


Notes: This figure shows two MOSFETs as switches.

In order to read out the array, Φ_{select} is turned on and this connects the source follower MOSFET amplifier to be connected to the readout line (the column bus).

Note that the MOSFET gate has an extremely high resistance, so there is no current flow from the photodiode to the rest of the circuit. Φ_{select} can be turned on and off without affecting the input voltage to the MOSFET. This is called "non destructive" read.

The MOSFET with V_{bias} at the gate acts as a resistor that controls the gain of the amplifier, which in the case of this application is close to unity.

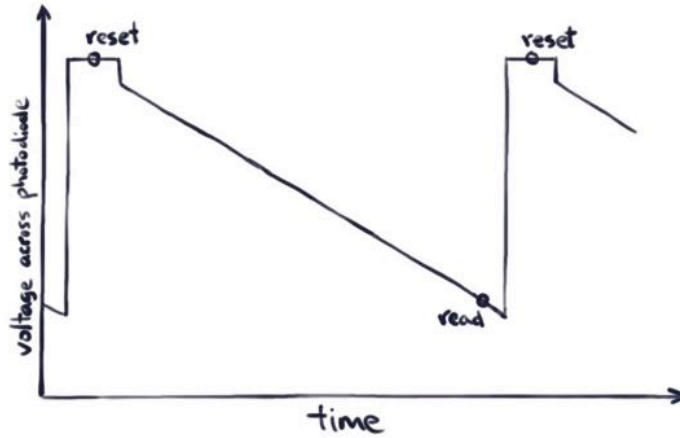


Notes: This figure shows two MOSFETs as switches.

It is remarkable that this circuit can operate at temperatures as low as 30K and provide detection down to a 3-5 electrons.

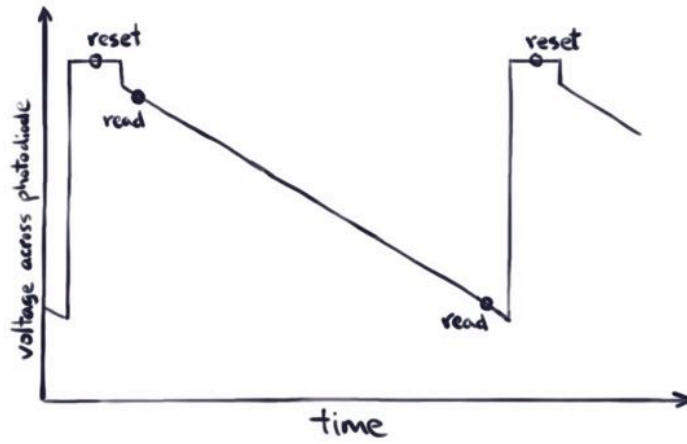
When the reset switch is closed the voltage across the photodiode increases as shown below. The switch is then opened and the signal current from the photodiode will discharge C_{det} . At the end of the integration period the source follower MOSFET is turned on to readout the voltage. Then the photo diode is reset again.

This is the simplest mode of reading the voltage, but it has a "kTC noise" component, which results from the thermal fluctuation of charges.



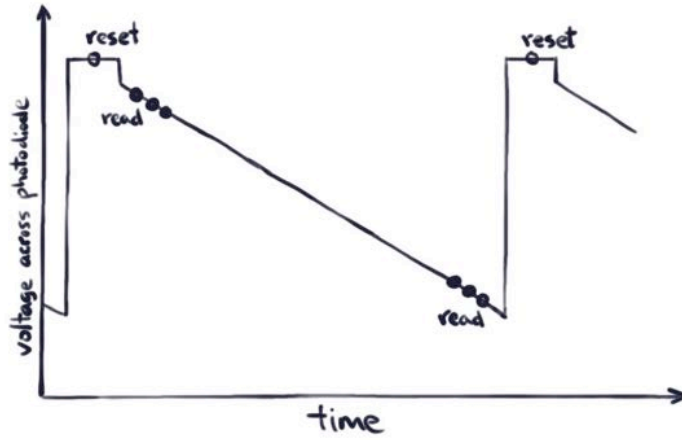
Notes:

In this readout mode, the voltage is measured right after the reset and at the end of the integration period. This is called "Double Correlated Sampling". It removes the KTC noise.



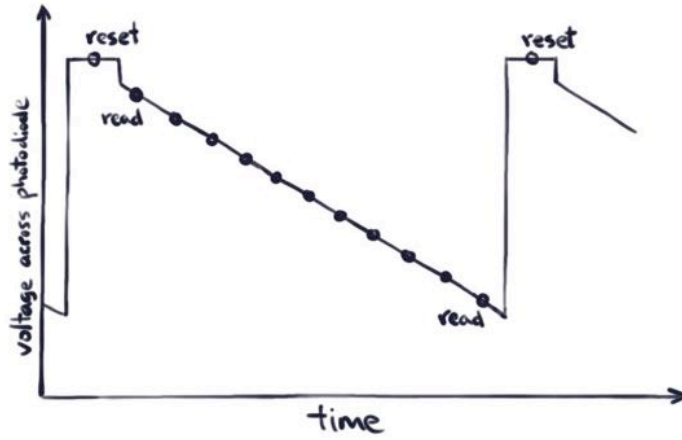
Notes:

A more effective readout mode is to do multiple reads at the beginning and end of the integration period. The difference of the average at the beginning and at the end is the signal. This is known as "Fowler sampling". The readout noise can be reduced approximately by the square root of n , where n is the number of reads.



Notes:

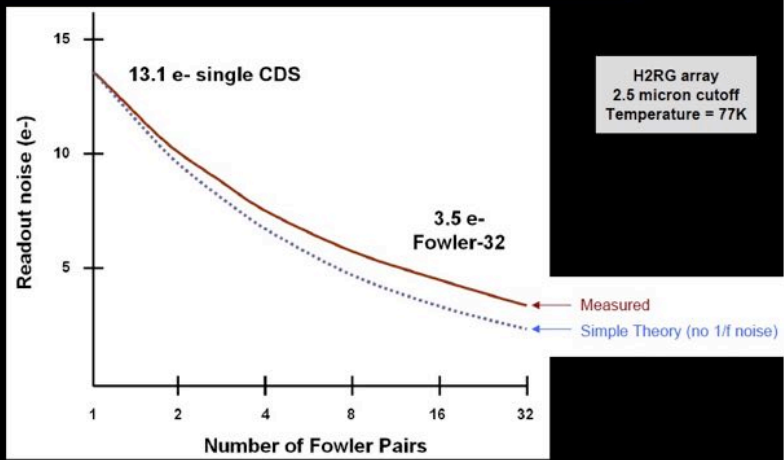
Another method is the read at a continuous rate while integrating. This is known as "sampling up the ramp". The slope of the line is fitted to get the signal current.



Notes:

Example of Noise vs Number of Fowler Samples

Non-destructive readout enables reduction of noise from multiple samples



Notes:

Typical array characteristics



Parameter	RVS VIRGO/VISTA	Teledyne H2RG JWST	RVS Orion	DRS Technologies WISE	RVS JWST
Detector type	HgCdTe	HgCdTe	InSb	Si:As IBC	Si:As IBC
Wavelength range (μm)	0.85–2.5	0.6–5.3	0.6–5.5	5–28	5–28
Format	2048 \times 2048	2048 \times 2048	2048 \times 2048	1024 \times 1024	1024 \times 1024
Pixel pitch (μm)	20	18	25	18	25
Operating temperature (K)	78	37	32	7.8	6.7
Read noise (e rms)	6 (slow readout)	6 (slow readout) 30–40 (fast readout)	6	42 (Fowler-1; lower noise expected with more reads)	10
Dark current (e/s)	<0.1	<0.01	0.01	<5	0.1
Well capacity (e)	> 1.4×10^5	8×10^4	1.5×10^5	> 10^5	2×10^5
Quantum efficiency	>70%	>80%	>80%	>70%	>70%
Outputs	4, 16	1, 4, 32	64	4	4
Frames/sec	0.4, 1.5	0.1 to 30	10	1	0.3
References	Love et al. (2004) Bezawada & Ives (2006)	Rauscher et al. (2004) Garnett et al. (2004)	McMurtry et al. (2003) Fowler et al. (2004)	Mainzer et al. (2005a)	Love et al. (2005)

Note: IBC, impurity band conduction; JWST, *James Webb Space Telescope*; RVS, Raytheon Vision Systems; VISTA, Visible and Infrared Survey Telescope for Astronomy; WISE, *Wide-Field Infrared Survey Explorer*.

Notes:

Rieke, G. H. (2007). "Infrared Detector Arrays for Astronomy." *Annual Review of Astronomy and Astrophysics* **45**: 77-115

Test results for JWST NIRSpec H2RG arrays.

Parameter	Req.	Unit	SCA serial number							
			17163	17280	17167	17169	17378	17168	17166	17195
NIRSpec SCA			491	492	N/A	N/A	N/A	N/A	N/A	N/A
Flight ranking			1	2	3	4	5	6	7	8
Mean dark current	<0.01	$e^- s^{-1} \text{pix}^{-1}$	0.0032	0.0041	0.0051	0.0027	0.0043	0.0032	0.0043	0.0047
Persistence ^a	<208	$e^- s^{-1}$	29	42	65	44	50	53	31	239
Total noise ^b	<6	$e^- \text{ rms}$	<4.32	<5.18	<4.8	<5.19	<5.07	<5.02	<4.46	<5.8
Mean DQE										
$0.6 < \lambda < 1 \mu\text{m}$	$\geq 70\%$	percent	79.5	80.4	78.9	83.9	86.5	75.8	89.4	81.5
$1 \leq \lambda < 5 \mu\text{m}$	$\geq 80\%$	percent	88.0	88.3	87.2	85.9	91.0	80.6	88.7	88.1
Pixel operability	$> 89\%$	percent	99.02	98.25	98.92	98.06	97.7	98.65	98.91	97.74
Pixel cross talk	<5%	percent	0.54	0.49	0.52	0.62	0.6	0.61	0.52	0.48
Test start date		MM/YY	08/13	09/13	08/13	09/13	11/13	10/13	10/13	11/13
Conversion gain		$e^- \text{ DN}^{-1}$	0.873	0.978	0.935	0.94	0.904	0.925	0.882	0.946
Transimpedance gain		$\mu\text{V per } e^-$	4.372	3.903	4.082	4.060	4.222	4.126	4.327	4.035
Read noise per CDS ^b		$e^- \text{ rms}$	<7.4	<8.9	<7.9	<9.1	<8.4	<8.3	<7.4	<8.8
Open pixels		pixels	470	63	7	0	0	863	1292	357
RTN pixels		%	3.3	4.0	2.3	4.3	3.6	3.2	2.7	3.6
Snowball rate		snowballs hr^{-1}	0.66	0.02	0.17	0.14	0.20	0.07	0.07	0.03
Bad rows		number	0	0	0	0	0	1	0	0
Void pixels		%	<1	0	1	<1	3	3	10	0
Cutoff wavelength		μm	5.45	5.37	5.42	5.44	5.47	5.32	5.41	5.36

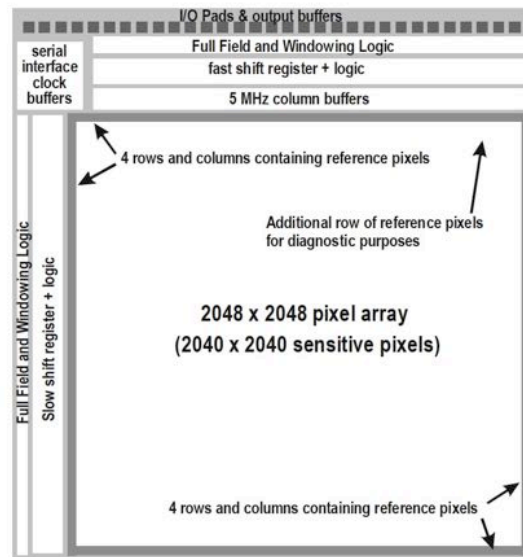
NOTE.— The two flight SCAs are indicated by boldface type.

Notes: This chart shows test results for the JWST NIRSpec H2RG arrays. Note the read noise and dark current. The quantum efficiency is between 0.8 and 1.0. These detectors are therefore nearly ideal.

Reference: Rauscher, B. J. et al. (2014). "New and Better Detectors for the JWST Near-Infrared Spectrograph." Publications of the Astronomical Society of the Pacific **126**: 739.

Layout of a HAWAII 2RG array (Loose et al. 2003). Note that there are reference pixels along the edge of the array. These are identical to a pixel but is not sensitive to photons. Therefore the reference pixels provide a way to reduce or eliminate noise sources that are common to all of the pixels.

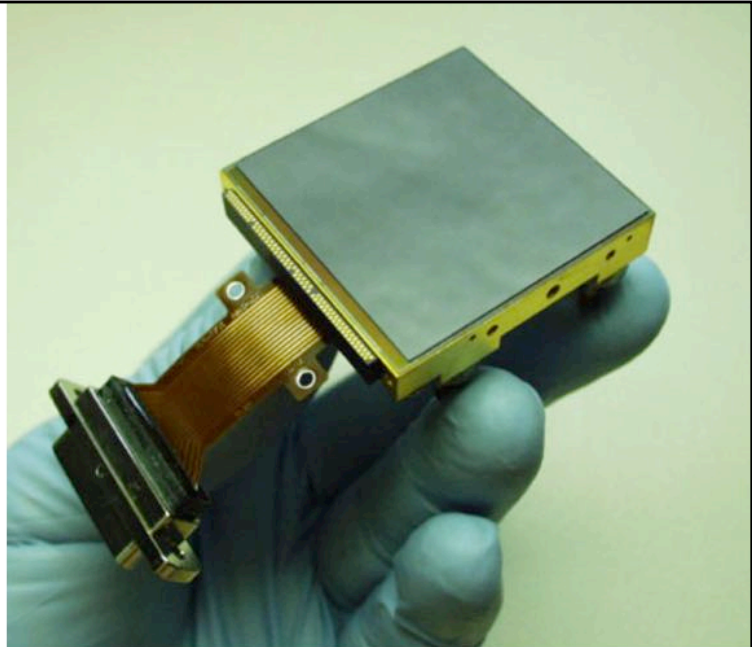
In this design the array can be placed next to two other arrays (two-side buttable). In another design the array can be placed next to three other arrays to minimize the gap between the arrays in large mosaics of detectors.



Notes: Reference: Loose, M. et al. (2003). HAWAII-2RG: a 2k x 2k CMOS multiplexer for low and high background astronomy applications. *IR Space Telescopes and Instruments*. J. C. Mather, SPIE. **4850**: 867-879.

Image of an infrared array with the readout cable attached (from Beletic et al. 2008). This is an H2RG-18 2Kx2K array for JWST and ground-based astronomy).

The electrical connector goes to an array controller that is either located outside the cryostat or located inside the cryostat next to the array.



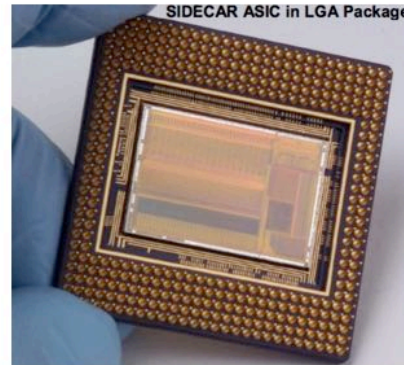
5-25

Notes: Reference: Beletic, J. W. et al. (2008). Teledyne Imaging Sensors: infrared imaging technologies for astronomy and civil space. High Energy, Optical, and Infrared Detectors for Astronomy III, SPIE. **7021**: 70210H.

Due to the need to reduce the power consumption for the JWST infrared detectors, an array controller was developed by Teledyne that was reduced to a single chip. It is called the SIDECAR ASIC. An ASIC is a term for a class of devices that are programmable and the acronym stands for "Application Specific Integrated Circuit". SIDECAR is an acronym that stands for "System Image, Digitizing, Enhancing, Controlling, and Retrieving". The SIDECAR ASIC is used to readout the array, digitize the signal, and to send the digital output to a computer for processing.

36 analog to digital channels
Clock signal generation
Programmable controller
Less than 300mW for 32 channel, 16-bit
sampling at 100 kHz
Requires one power supply and one master
clock for operation

Note: 8mW of power for JWST application.

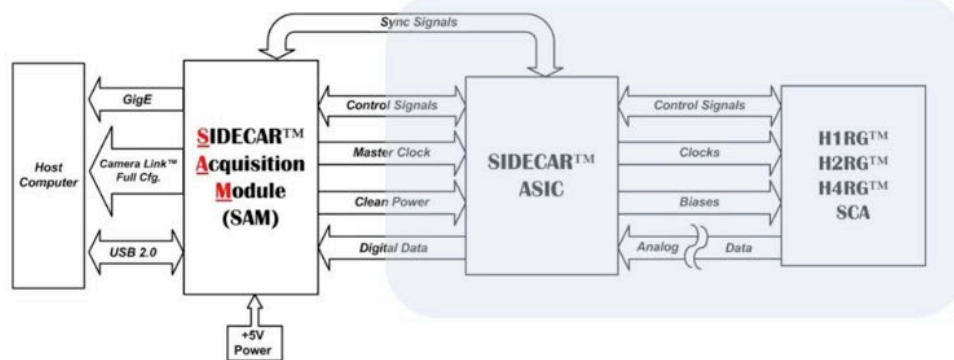


5-26

Notes: Reference: http://www.teledyne-si.com/pdf/SIDECAR%20ASIC%20Dev%20Kit%20Brochure%20-%20Jan_2017_V1.0.pdf

This is the specs for a ground-based application. For JWST the SIDECAR ASIC dissipates less than 8 mW of power.

This is a diagram showing the major components of the HxRG family of arrays. “SCA” stands for Sensor Chip Assembly and consists of the the detector array and the readout multiplexer (also known as the ROIC).



Block diagram showing the data and signal flows

A. Tokunaga, Introduction to Infrared Astronomy, Univ. of Tokyo
Visiting Professor Lecture, Feb. 2018

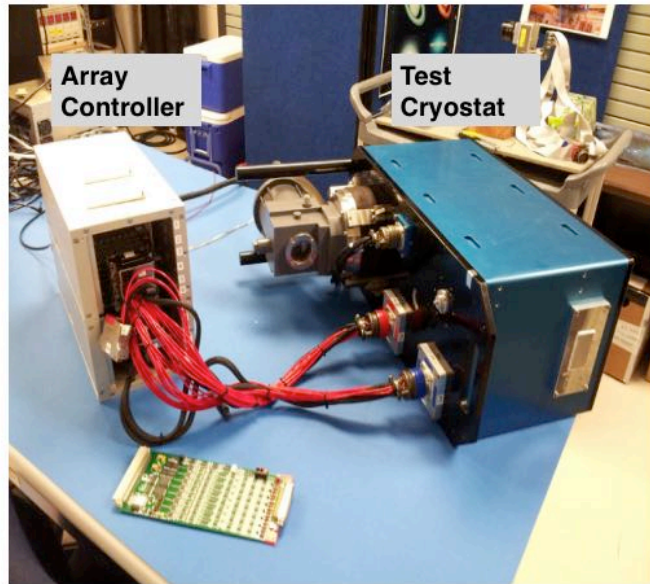
5-27

Notes: Reference: http://www.teledyne-si.com/pdf/SIDECAR%20ASIC%20Dev%20Kit%20Brochure%20-%20Jan_2017_V1.0.pdf

Blue shaded area shows the cryostat. The detector (SCA) and the ASIC are cooled inside of the cryostat. The ASIC is controlled by the host computer through an interface card called the SIDE CAR Acquisition Module.

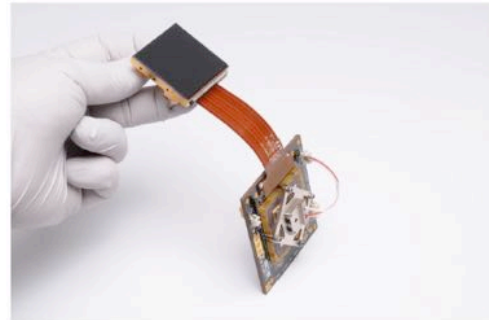
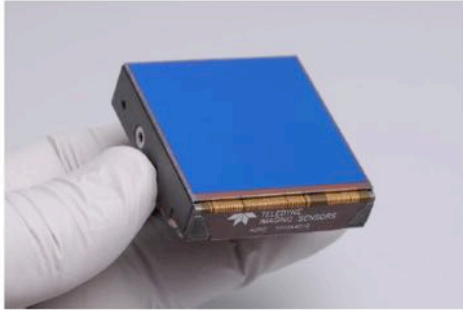
This shows another type of array controller that does not use the SIDECAR ASIC. The array controller is outside of the cryostat. The analog signals from the array is carried out of the cryostat to the array controller where it is digitized.

Both the ASIC and the external array controller can give similar performance. The advantage of the external array controller is that more customization is possible by the engineers who built it. The ASIC has the advantage of being more compact, using less power, and it does not dissipate heat into the dome.



Notes: Image shown is a H2RG array controller built at the NASA Infrared Telescope Facility.

The HAWAII 2RG (H2RG) arrays were specifically designed and built for the three near-infrared instruments on JWST. There are a total of 15 H2RG arrays using the SIDECAR ASIC installed on JWST. The H2RG arrays will also be used on the ESA Euclid spacecraft. In addition they are used on many ground-based observatories.



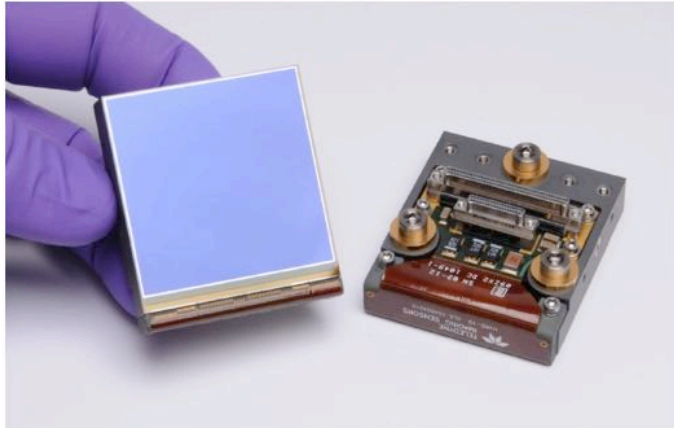
Notes: Images from Teledyne and D. Hall.

University of Hawaii-Teledyne Imaging Systems 'HAWAII' Heritage



Notes: This slide shows the progression of HgCdTe array development to ever larger arrays and capability (D. Hall, private communication). The principal investigator for these arrays is Donald Hall at the Institute for Astronomy, University of Hawaii. He worked closely with Teledyne Imaging Systems since 1994 to develop these arrays.

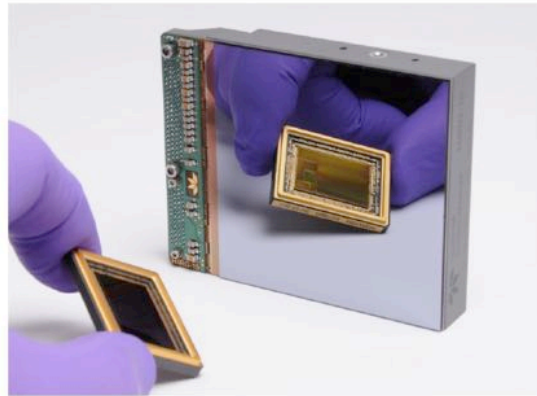
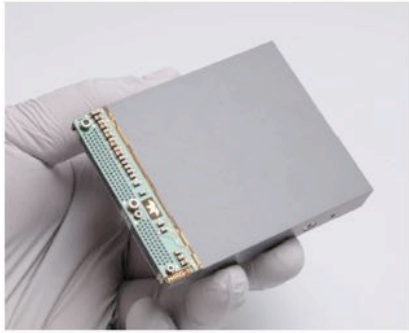
The HAWAII 4RG-10 is being developed for the WFIRST-AFTA mission. It is planned to have 18 H4RG arrays in a 3x6 format.



A. Tokunaga, Introduction to Infrared Astronomy, Univ. of Tokyo
Visiting Professor Lecture, Feb. 2018

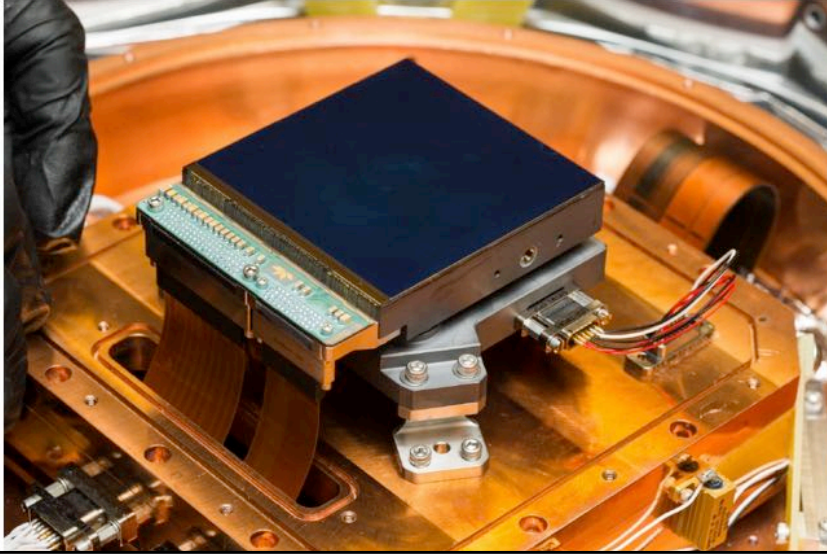
Notes: Images from Teledyne and D. Hall.

The HAWAII 4RG-15 array was developed from ground-based astronomy under a Univ. of Hawaii/Teledyne partnership. These arrays have been purchased by the Subaru Telescope, Canada-France-Hawaii Telescope, and the European Space Observatory.



Notes: Images from Teledyne and D. Hall.

The H4RG-15 array mounted in ULBCam, a wide-field camera built for the Univ. of Hawaii 2.2-m telescope. This close up photo shows the details of mounting the array into an actual camera.



5-33

Notes: Photo from D. Hall.

Infrared Mosaics



HgCdTe 2K x 2K, 18 μ m pixels

2x2



HgCdTe 4K x 4K mosaic, 18 μ m pixels

Teledyne Imaging Sensors

Notes:



Notes: